



# Reservoir Properties of The Jurassic Khatatba Formation: Tut Oil Field, NW-Desert, Egypt

Abdel Mektader A. El Sayed<sup>1)</sup>, Nahla A. El Sayed<sup>2\*)</sup>, A. A. Radwan<sup>3)</sup>

<sup>1\*)</sup> Geophysics Department, Faculty of Science, Ain Shams University, Cairo, Egypt

<sup>2\*)</sup> Egyptian Petroleum Research Institute, Exploration Department, Nasr City, Egypt; email: muktader76@yahoo.com

<sup>3)</sup> Khalda Petroleum Company (Apache J.V.), P.O Box 560, Maddi, Cairo, Egypt

<http://doi.org/10.29227/IM-2024-01-13>

Submission date: 11.4.2023 | Review date: 1.5.2023

## Abstract

The Tut oil field is in the North-western part of the Western Desert. This work aims to study the reservoir characteristics, to evaluate the hydrocarbon potentiality of the Upper and Lower Safa Members based on the available subsurface data obtained from open-hole well log records of four wells distributed in the study area. Numerous isopach and lithofacies maps have been constructed. The petrophysical evaluation, in terms of determining reservoir net-pay thickness, shale content (Vsh), effective porosity ( $\phi_{eff}$ ), water saturation ( $S_w$ ) and hydrocarbon saturation ( $S_h$ ), were estimated. The vertical and the lateral distribution of the reservoir characteristics, in the form of litho-saturation cross-plots, iso-parametric maps and lithologic-matrix cross-plots were constructed. Three hydrocarbon charged zones in the Khatatba Formation were defined and represented by the Upper Safa-Top, Upper Safa-Bottom and Lower Safa-Top. The upper most part of Upper Safa Member (Upper Safa-Top) reservoir represents an oil producing zone where it consists of shallow marine to alluvial sediments. The Lower most part of Upper Safa Member (Upper Safa-Bottom) reservoir represents gas producing zone where it consists of a thick alluvial sand body. Finally, the upper most part of Lower Safa Member (Lower Safa-Top) reservoir represents an oil-gas producing zone consisting of shallow marine sediments with high terrestrial input. The iso-parametric maps show that Northern and central parts of the study area are the most favorable parts for hydrocarbon accumulation due to the increase in net-pay thickness and average effective porosity and decrease in water saturation toward these parts.

*Keywords: reservoir, hydrocarbon, khatatba formation, oil field, porosity, egypt*

## Introduction

The stratigraphic sequence in the northern Western Desert is characterized by several major transgressive/regressive cycles on the platform margin. The Mesozoic sequence unconformably overlies the rocks. The Mesozoic stratigraphic succession is much better understood than the Paleozoic one, as indicated by [1-7]. The Upper Cretaceous Bahariya Formation is one of the major hydrocarbons producing zone in the northern part of the western desert. It is studied petrophysically by [8, 9]. The Tut oil field (Figure 1a) is in the Northern part of the Western Desert. This area is the most prolific petroleum province in Egypt. [10] stated that one of the main producing reservoirs in this province is the Middle Jurassic Khatatba Formation (Figure - 1b). According [11] the sedimentary section in the northern part of the Western Desert was subdivided into three parts: the lower clastic unit (from Cambrian to pre-Cenomanian), the middle carbonates, (from Cenomanian to Eocene) and the upper clastic unit, (from Oligocene to Recent). The depositional environment of the Khatatba Formation is detected as marine to fluvio-marine sediments. Many structural controls are playing great roles in hydrocarbon entrapment. [12] stated that most of the Western Desert oil production comes from the Northern basins, including Matruh – Shushan basins (70% up to 90%) from the Jurassic- Cretaceous sands.

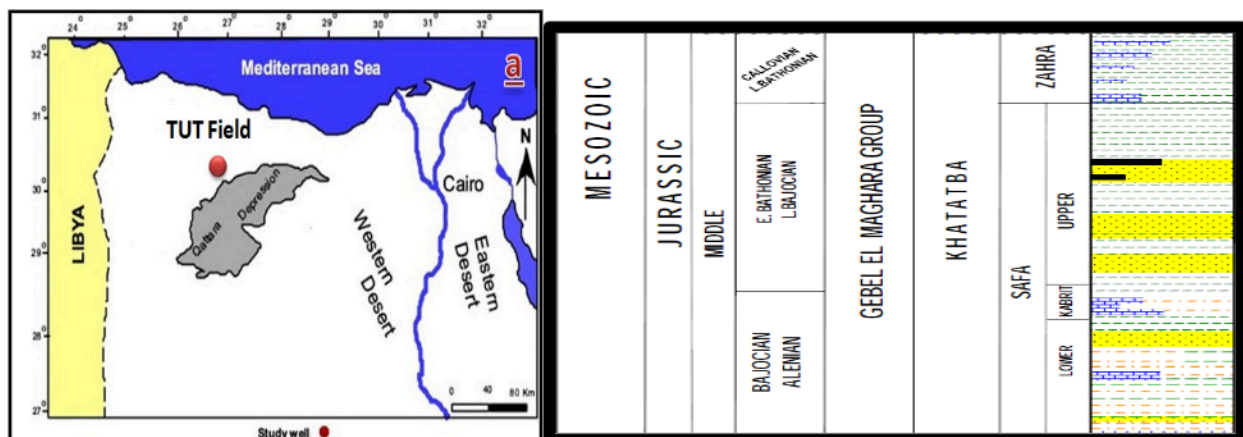


Fig. 1. Location map of the study area (as Figure 2), Study well, Stratigraphic Position of the Khatatba Formation (as Figure 3) [13]

Use 10 pt Times new Roman font, and indent the first line: 0.2", justified. State the objectives of the work and provide an adequate background, avoiding a detailed literature survey or a summary of the results.

## Methodology

The bore-hole logs of four drilled wells (TUT-48, TUT-25, TUT-84, and TUT-57) in the study area have been used to achieve the present study. They are represented by resistivity, calliper, spontaneous potential, gamma-ray, density ( $\rho$ ), neutron ( $\Phi$ ) and Sonic logs ( $\Delta T$ ). The petrophysical evaluation is performed using I.P. version 3.6, Petrel software. The petrophysical characteristics are illustrated in both areal (iso-parametric maps) and vertical distribution (in the form of litho-saturation cross-plots). Before calculation operations, corrections were carried out to keep away the effects of some un-wanted parameters and corrected for lithology, mud weight, borehole diameter and formation temperature. The corrected data have been used to determine the petrophysical properties of the geological intervals that could have high potential hydrocarbon zones within the target- Safa Member. It has been carried out as the following sequence.

### Determination of Formation Temperature

The borehole temperature at any depth is calculated using the following equation.

$$FT = ST + \{D * (BHT - ST) / TD\} \quad (1)$$

where: FT is the formation temperature ( $^{\circ}F$ ), ST is the mean surface temperature ( $^{\circ}F$ ), D is the depth of the formation (feet), BHT is the borehole temperature ( $^{\circ}F$ ) and TD is the total depth (feet) of well.

The determination of Mud Filtrate Resistivity was performed as:

$$R_{mfc} = R_{mf} * \{(ST + 6.77) / (FT + 6.77)\} \quad (2)$$

where:  $R_{mfc}$  is the resistivity of mud filtrate at the studied formation (ohm-m) and  $R_{mf}$  is the resistivity of mud filtrate at the surface from log heading (ohm-m).

### Determination of Shale Volume (Vsh):

The estimation of shale volume is a very important task in well log analysis because the interpretation problem in shaly formations is the calculation of porosity and saturation free from the shale effect. In the present study, the method of single curve shale indicator was applied, to obtain the shale volume in the Safa Formation. In this method, only one log type (gamma-ray, neutron, or resistivity) is used to calculate the volume of shale.

#### Gamma-ray method

The shale volume (Vsh), is calculated using the following equation [14]:

$$V_{sh} = 0.33 [2(2 * IGR) - 1] \quad (for\ older\ rocks) \quad (3)$$

where the  $I_{GR}$  is the gamma-ray index and can be determined by the following equation:

$$IGR = (GR\ log - GR\ cl) / (GR\ sh - GR\ cl) \quad (4)$$

where: GR log is the gamma-ray log reading, GR cl is the gamma-ray of clean rocks and GR sh is the gamma-ray of shale bed.

#### Neutron method

The Vsh calculated from neutron log, is defined as follows (Schlumberger, 1974).

$$V_{sh} = \Phi\ N\ log / \Phi\ N\ sh \quad (5)$$

where:  $\Phi\ N\ log$  is the neutron log reading and  $\Phi\ N\ sh$  is neutron of shale bed.

#### Resistivity method

The  $V_{sh}$  can be calculated from the resistivity log, through following equation.

$$V_{sh} = (R_{Sh} / R_t) 1/b \quad (6)$$

where:  $R_t$  is the true resistivity log reading,  $R_{Sh}$  is the resistivity of shale and  $b$  is a constant, depending on the ( $R_{Sh} / R_t$ ) ratio as  $b = 2$ , if ( $R_{Sh} / R_t$ )  $< 0.5$  and  $b = 1$ , if  $0.5 < (R_{Sh} / R_t) < 1$ . Generally, the calculated shale volume from the gamma-ray method is the most reliable as it gives the lowest values of  $V_{Sh}$ , compared to those of the neutron and resistivity methods. These applied methods may be affected by other factors, such as the presence of radioactive minerals and borehole conditions, so the correlation among the three  $V_{Sh}$  curves helps to select the minimum value of  $V_{Sh}$  at every depth.

### Porosity Determination

Porosity is the most important property for reservoir rocks. Porosity values can be obtained from different logging tools, as sonic, formation density and/or neutron log. Combination of two or three porosity tools gives better results, lithology, and formation characteristics, than those obtained from a single tool.

### Porosity determination from density log:

Porosity ( $\Phi_D$ ) is derived from the bulk density in clean formation, using the following formula.

$$\Phi D = (\rho_{ma} - \rho_{log}) / (\rho_{ma} - \rho_f) \quad (7)$$

where:  $\rho_{ma}$  is the matrix density,  $\rho_{log}$  is the density log reading and  $\rho_f$  is the density of mud fluid.

In the present study, the matrix density ( $\rho_{ma}$ ) equals 2.65 and 2.7 gm/cc for the Upper and Lower Safa Members, respectively. The obtained porosity was corrected to eliminate the shale effect, as follow.

$$(\Phi D)C = \Phi D - (V_{Sh} \cdot \Phi DSh) \quad (8)$$

$$\text{where: } \Phi DSh = (\rho_{ma} - \rho_{Sh}) / (\rho_{ma} - \rho_f)$$

#### Porosity determination from neutron log:

The neutron porosity ( $\Phi_N$ ) is corrected to eliminate the effect of shale, using the following equation.

$$(\Phi N)C = \Phi N - (V_{Sh} \cdot \Phi NSh) \quad (9)$$

where:  $\Phi_{NSh}$  is the neutron reading of shale bed.

#### The effective porosity determination:

The combination of the corrected density porosity ( $\Phi_D$ ) C and the corrected neutron porosity ( $\Phi_N$ )C was useful to obtain the effective porosity ( $\Phi_{eff}$ ). In oil-bearing zones, ( $\Phi_N$ ) C is greater than ( $\Phi_D$ )C while the following formula is applied.

$$\Phi_{eff} = \{(\Phi_N)C + (\Phi_D)C\} / 2 \quad (10)$$

When the formation contains gas, ( $\Phi_D$ ) C will be greater than ( $\Phi_N$ ) C. The effective porosity can be calculated, using the following equation [13].

$$\Phi_{eff} = \{((\Phi_N)C^2 + (\Phi_D)C^2) / 2\}^{1/2} \quad (11)$$

#### Saturation Determination

The saturation of formation fluid is determined by different methods with their modifications, which are all based on the work done by [6, 15, 16].

#### Water saturation determination

Water saturation is often determined from the logging measurement of resistivity and the knowledge of porosity, water resistivity and shale volume. [13] introduced the most common used equation in oil industry, that calculates the water saturation in the uninvaded zone, with respect to shale effect as follows:

$$S_w n/2 = (1/(R_t)1/2) / \{(V_{Sh} (1 - V_{Sh}/2) / (R_{sh})1/2) + (\Phi m/2 / (a \cdot R_w)1/2)\} \quad (12)$$

where:  $R_w$  is the formation water resistivity,  $R_t$  is the resistivity reading in the uninvaded zone, (n) is the saturation exponent, (a) is Archie's multiplier and (m) is the cementation factor.

In this study, the value 0.017 ohm-m @ 260° F was used for  $R_w$ , according to the measured  $R_w$  values from Sp-curves, for the Khatatba (Safa) Formation in some bore holes in the Khaldia Petroleum Company. The same equation for  $S_w$  calculation, is used to estimate the water saturation in the flushed zone ( $S_{xo}$ ) by replacing  $R_t$  and  $R_w$  with  $R_{xo}$  and  $R_{mf}$ , respectively.

#### Hydrocarbon saturation determination:

The fundamental equation for calculating hydrocarbon saturation ( $Sh$ ) is  $Sh = 1 - S_w$ . The hydrocarbons can be differentiated into residual ( $S_{hr}$ ) and movable ( $S_{hm}$ ) saturations. In simple forms, both movable and residual hydrocarbons can be calculated as.

$$S_{hr} = 1 - S_{xo} \quad \text{and} \quad S_{hm} = Sh - S_{hr} \quad (13)$$

## Results and Discussions

Petrophysical analysis has been carried out to evaluate and delineate the most effective sand zones with fluid contents in the Safa Members. In this study of the Jurassic Safa Members, that divided into three interesting reservoirs: (Upper Safa-Top, Upper Safa-Bottom and Lower Safa-Top). The net-pay zones, gross thickness, effective porosity, water saturation and hydrocarbon saturation in the pore spaces were calculated. The petrophysical characteristics and lithologies are constructed vertically in the form of litho-saturation cross-plots, and laterally in the form of iso-parametric maps (Figure 4 -9).

#### Petrophysical Evaluation

The litho-saturation cross-plots are constructed to illustrate the gross characters of the petrophysical parameters, in terms of lithology fractions and fluid saturations throughout the wells in the vertical direction, as shown in Figure 10. According to the obtained parameters, the best location for hydrocarbon accumulation, that included in the Upper Safa-Top Member, is laying at the central part of the study area and North direction. while the best location for hydrocarbon accumulation, that included in the Upper

Safa-Bottom Member, is laying at N and NE directions. Finally, the best location for hydrocarbon accumulation, that included in the Lower Safa-Top Member, is laying at W- direction and the central part of the study area.

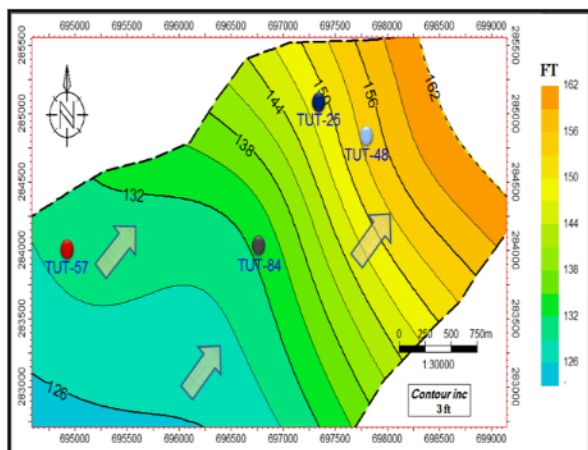


Fig.4a): Total thickness map of the Upper Safa-Top

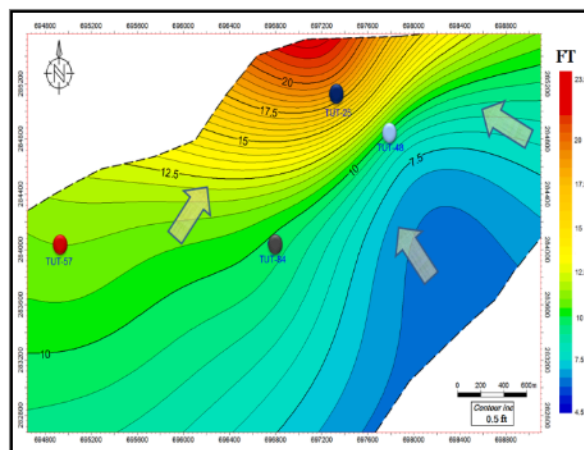


Fig.5a): Shale volume map of the Upper Safa-Top

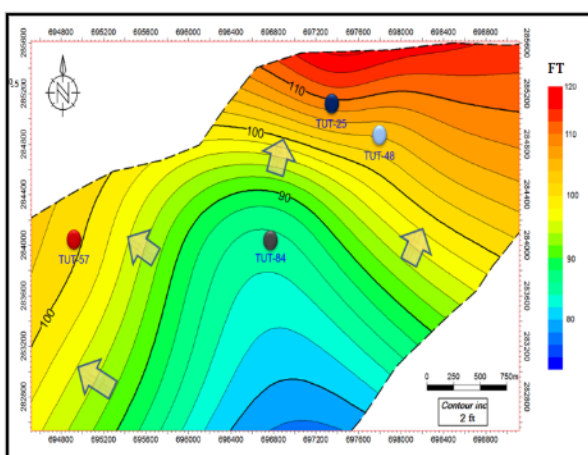


Fig.4b): Total thickness map of the Upper Safa-Bottom reservoir.

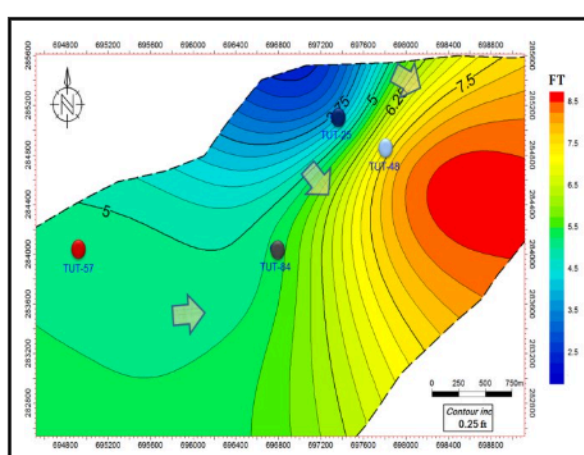


Fig.5b): Shale (Vsh,%) map of the Upper Safa-Bottom

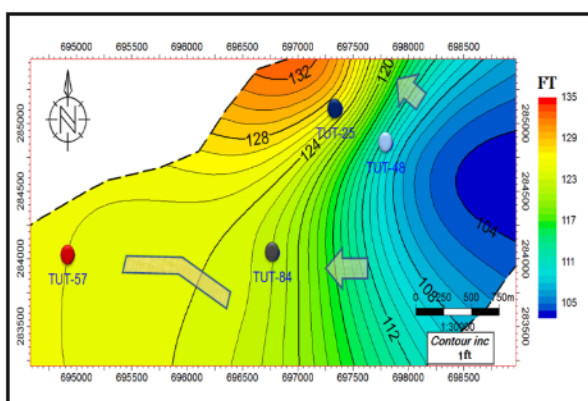


Fig.4c): Total thickness map of the Lower Safa-Top

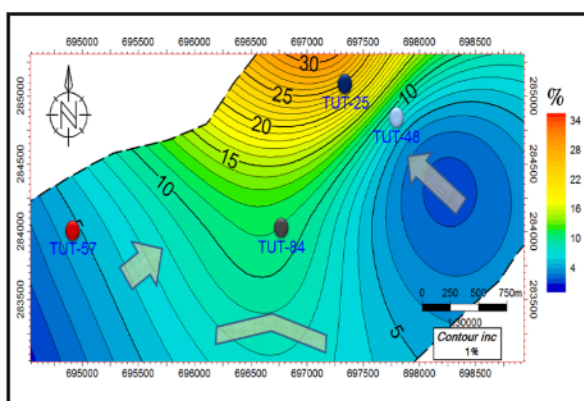


Fig.5c): Shale (Vsh,%) of Lower Safa-top

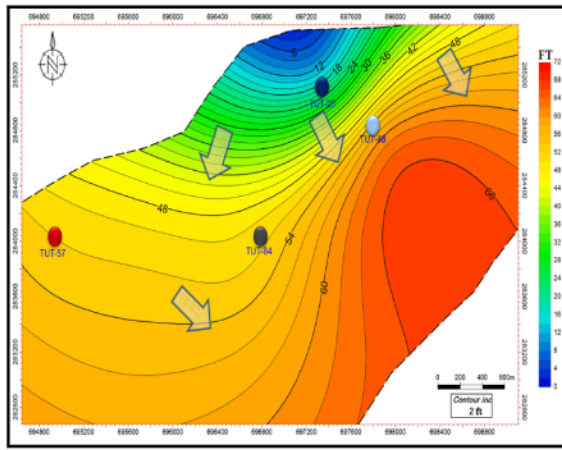


Fig 6a): Net pay map of the Upper Safa-Top reservoir

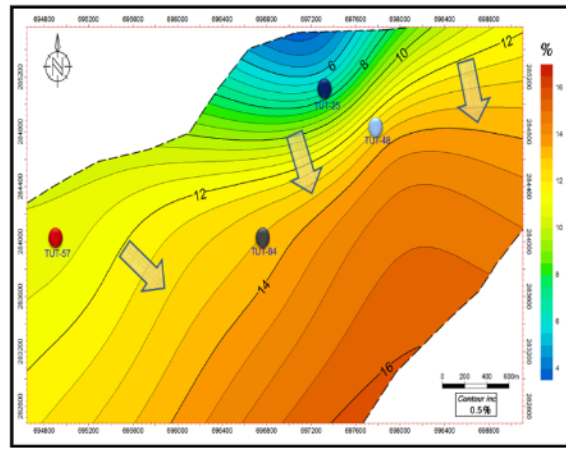


Fig.7a): ( $O_{eff}$ ,%) map of the Upper Safa-Top reservoir.

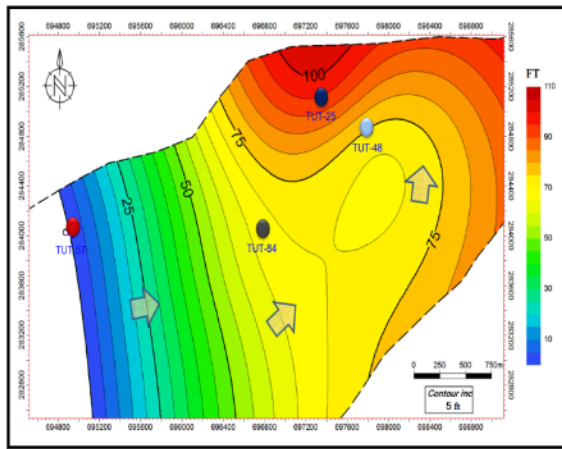


Fig 6b): Net pay map of the Upper Safa- Bottom reservoir.

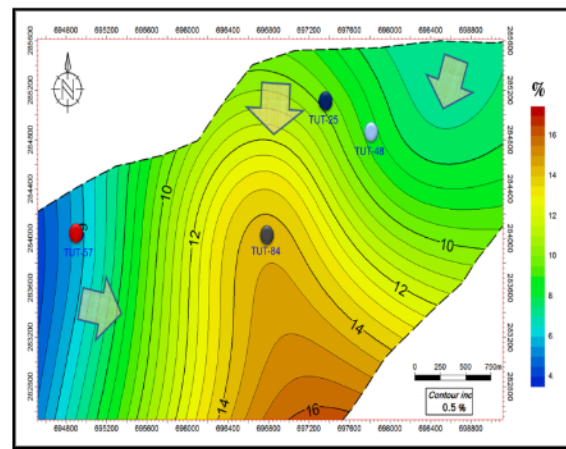


Fig.7b): ( $O_{eff}$ ,%) map of the Upper Safa-Bottom

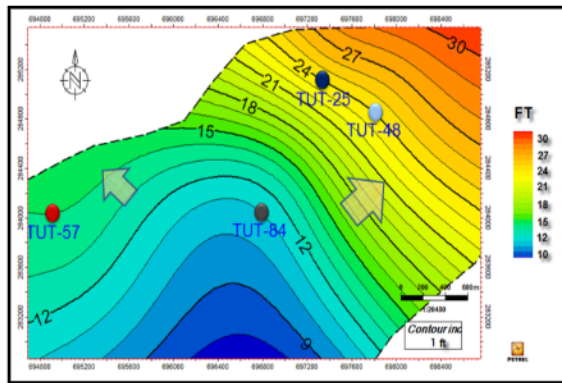


Fig 6c): Net pay map of the Lower Safa-Top reservoir.

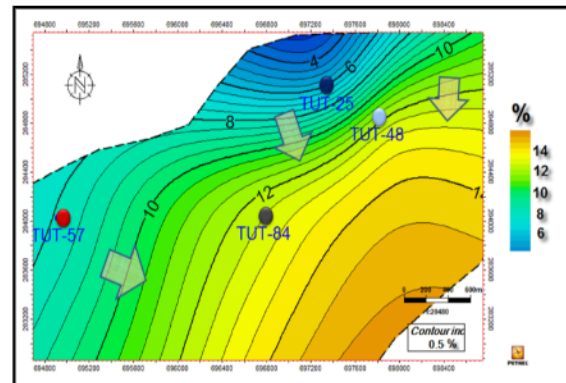


Fig.7c): ( $O_{eff}$ ,%) map of the Lower Safa-Bottom

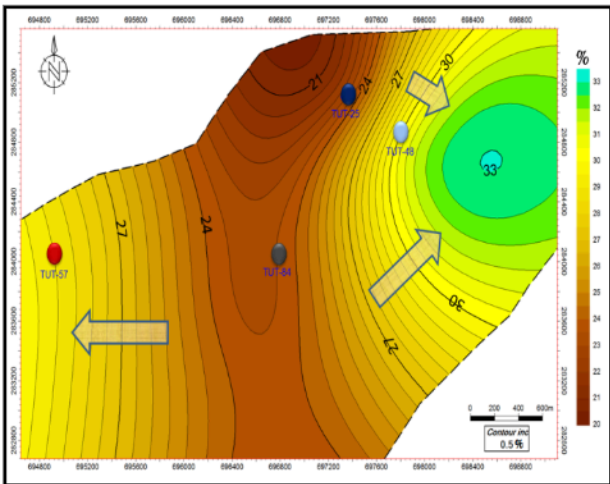


Fig. 8a. (Sw;% ) map of the Upper Safa-Top

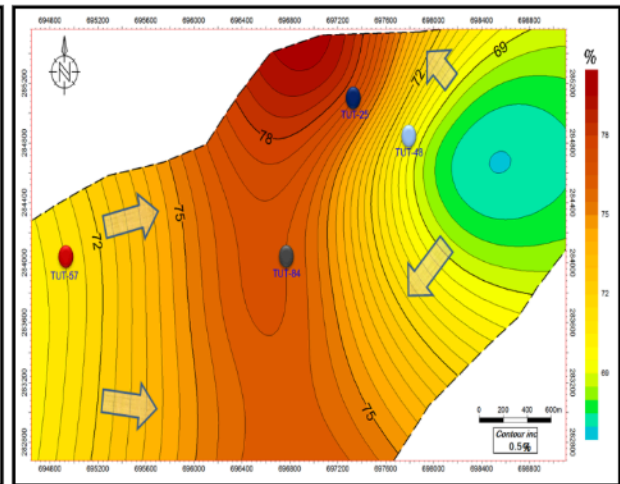


Fig. 9a. (Sh;% ) map of the Upper Safa-Top

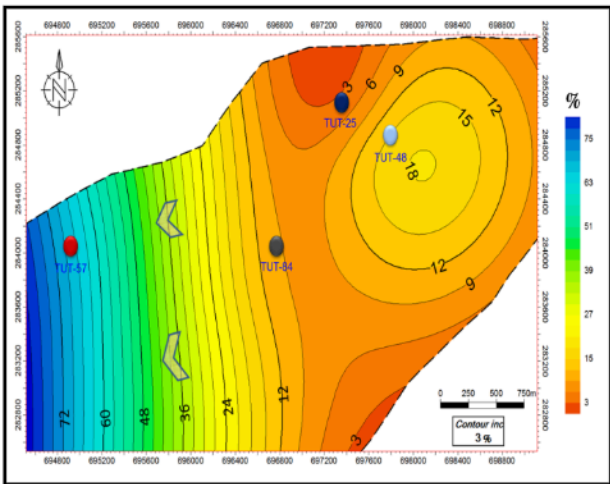


Fig. 8b. (Sw;% ) map of the Upper Safa- Bottom

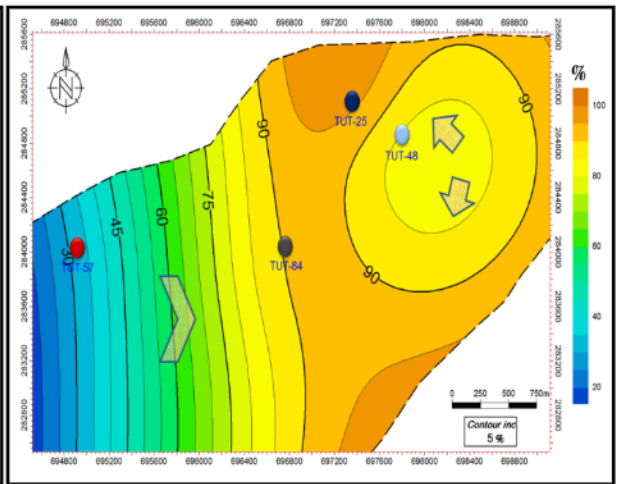


Fig. 9b. (Sh;% ) map of the Upper Safa- Bottom

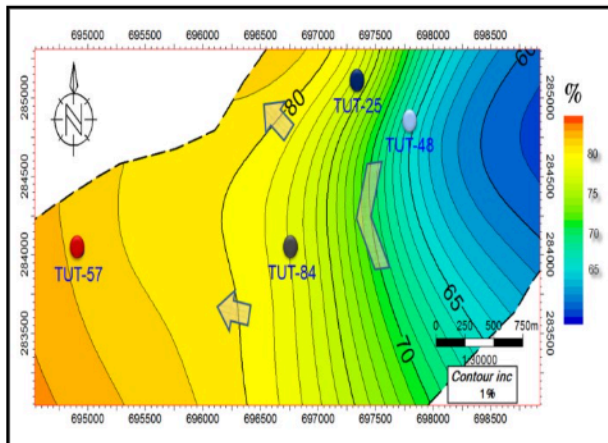


Fig. 8c. (Sw;% ) map of the Lower Safa- Top

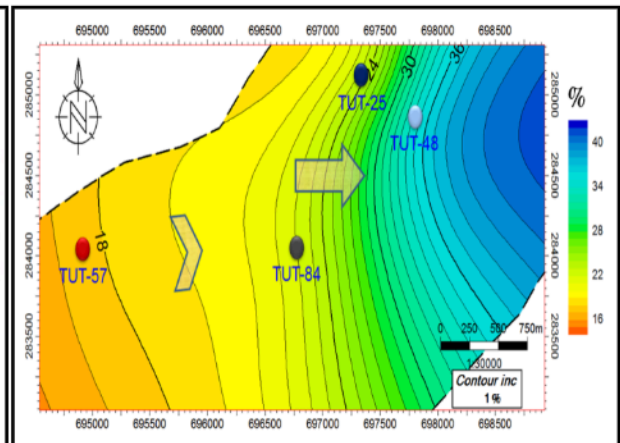


Fig. 9c. (Sh;% ) map of the Lower Safa bottom

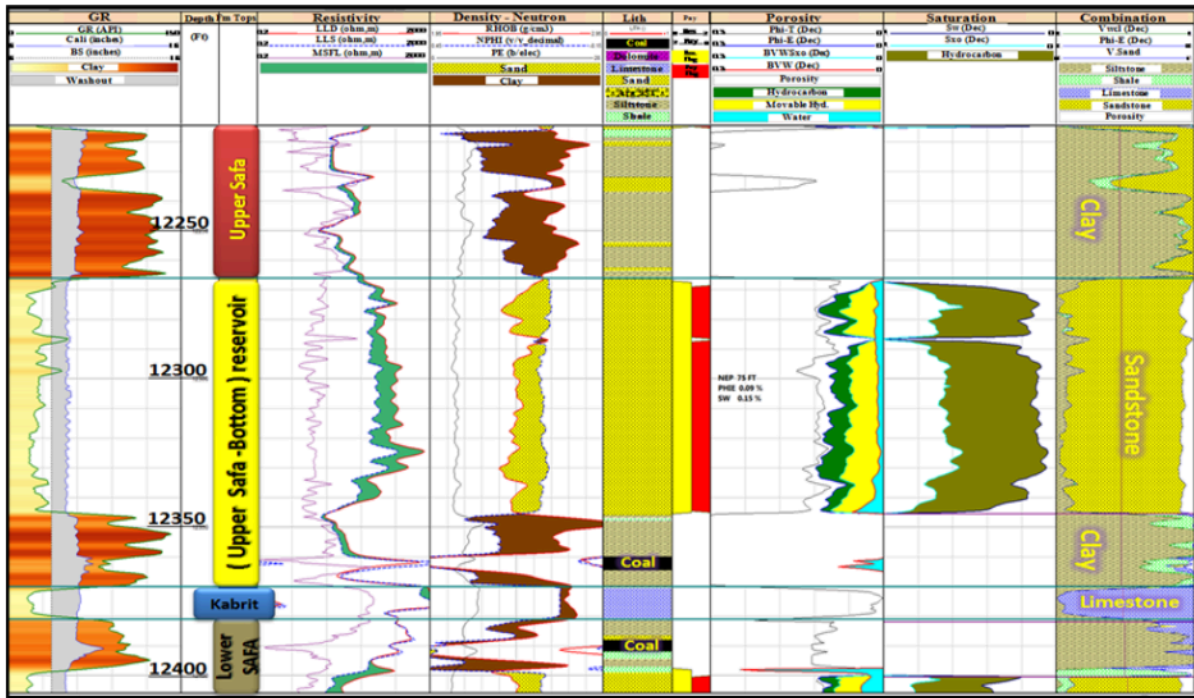


Fig. 10. Litho-saturation cross-plots illustrates the gross characters of the petrophysical parameters, in terms of lithology fractions and fluid saturations throughout the well in the vertical direction.

### Conclusions

The calculated average porosity of the Upper Safa-Top reservoir is 8.5%. The reservoir is sandstone, with bulk density ranging from 2.28 to 2.65 g/cc, which indicates the combination of the argillaceous and slightly calcareous cements. The fluid analysis reveals that the formation saturated with hydrocarbons ranges from 70% to 77% in TUT-48 and TUT-84 wells, respectively. The calculated average porosity of the Upper Safa-Bottom) reservoir is 9.65%. The reservoir is sandstone, with the bulk density ranging from 2.24 to 2.50 g/cc, which indicates the combination of siliceous and argillaceous cements. The fluid analysis reveals that the formation is saturated with hydrocarbons reaches 90% to 96% in TUT-25 and TUT-84 wells, respectively.

The Lower Safa-Top reservoir has an average porosity of 9.8%. The reservoir is sandstone, with the bulk density ranging from 2.3 to 2.65 g/cc, which indicates the combination of the argillaceous and slightly calcareous cements. The fluid analysis reveals that, the formation is saturated with hydrocarbons, which reaches 78% in TUT-84 wells. The obtained results could be indicating that the Northern and central parts of the study area are the most favourable for hydrocarbon accumulation and production, due to the increase in its net-pay thickness and average effective porosity and decrease in water saturation.

### Acknowledgment

Authors wishing to acknowledge Petrophysical Research Unit of Ain Shams University and EGPC and Apache Oil Company for data providing and permission of publication.

## References

1. A.S. Abdine, Deibis, S., 1972, Lower Cretaceous-Aptian sediments and their oil prospects in the Northern Western Desert, Egypt. 8th Arab Petrol. Conf., Algiers. No. 74 (B-3), 17 p.
2. W.M. Meshref., 1982. Regional structural setting of Northern Egypt. EGPC 6th Expl. Sem., Cairo, 11p.
3. W.M. Meshref, Abdel Baki, S. H., Abdel Hady, H. M. and Soliman, S. A., 1980. Magnetic trend analysis in Northern part of Arabian-Nubian Shield and its tectonic implications. Ann. Geol. Survey, Egypt, 10, 939-953.
4. M. Abu El Naga, 1984. Paleozoic and Mesozoic depocenters and hydrocarbon generating areas, Northwestern Desert. EGPC 7th, Expl. Sem. Cairo, 8 p.
5. S. Moussa, 1986. Evaluation of the sedimentary basins of the Northern Western Desert, Egypt. EGPC 8th Expl. Sem. Cairo, 14 p.
6. Schlumberger, 1972-1995. Log interpretation Vol. I-Principles/Applications, p. 113-243
7. M.G. Barakat Darwish, M. and Abdel Hamid, M. L., 1987. Hydrocarbon source rock evaluation of the Upper Cretaceous (Abu Roach Formation) east Abu Gharadiq area, Northwestern Desert, Egypt. M. E. R. C. Ain Shams University, Earth Sci., Ser. 1, 120-150.
8. Schlumberger, 1972-1995. Log interpretation Vol. I-Principles/Applications, p. 113-243
9. A.A. El-Khadragy, A.A., Shazly, T.F., Ramadan M. and El-Sawy, M.Z., 2016, Petrophysical investigations to both Rudeis and Kareem formations, Ras Ghara oil field, Gulf of Suez, Egypt. Egyptian Journal of Petroleum (2016).
10. J. Dolson, Shann, M., Matbouly, S., Harwood, C., Rashed, R. and Hammouda, H. 2001. The petroleum potential of Egypt. In: Downey, M., Threet, J. and Morgan, W. (eds.). Petroleum Provenance of the Twenty-first Century, American Association of Petroleum Geologist., Mem. 74, p. 453-461.
11. A. Abu Shady, El-Shishtawy, A.M, A. T. Abdel Hameed and Abdel Kader, T.A Proc. 6th International Symposium on Geophysics, Tanta, Egypt (2010), 34-46.
12. H. Metwalli, Saad, M. and Ali, T. 2000. Effect of depositional environments on reservoir capacity of Upper Baharyia Formation, Meleiha Oilfields, Northwestern Desert, Egypt. Journal of the Sedimentological Society of Egypt, V. 8a.
13. Khalda Oil Co. (Personal communications).
14. Dresser Atlas, 1979. Log interpretation charts. Dresser Industries Inc., Huston, Texas, 107 p.
15. A. Poupon, and Leveaux, J., 1971, Evaluation of Water Saturation in shaly Formation," Trans., 11th Ann. SPWLA Logging Symposium.
16. G.E. Archie, 1942. The electrical resistivity log as an aid in determining some reservoir characteristics. Trans., AIME, 146, 54-67.